Article

Not peer-reviewed version

Long-Term Corrosion Behavior of Y-TZP Dental Ceramics

Lidija Ćurković * , Sanja Štefančić , Irena Žmak * , Vilko Mandić , Ivana Gabelica , Ketij Mehulić

Posted Date: 17 July 2025

doi: 10.20944/preprints202507.1480.v1

Keywords: Y-TZP ceramics; dental ceramic; chemical stability; corrosion rate constant

 doi:10.20944/preprints202507.1480.v1

Article

Long-Term Corrosion Behavior of Y-TZP Dental Ceramics

Lidija Ćurković [1,*], Sanja Štefančić [2], Irena Žmak [1,*], Vilko Mandić [3], Ivana Gabelica [1] and Ketij Mehulić [4]

[1] University of Zagreb, Faculty of Mechanical Engineering and Naval Architecture, Ivana Lučića 5, 10000 Zagreb, Croatia
[2] MarisaDENT, Dugi dol 25, 10000 Zagreb, Croatia
[3] University of Zagreb, Faculty of Chemical Engineering and Technology, Trg Marka Marulića 19, 10000 Zagreb, Croatia
[4] University of Zagreb, Department of Fixed Prosthodontics, School of Dental Medicine, Gundulićeva 5, 10000 Zagreb, Croatia
* Correspondence: lidija.curkovic@fsb.unizg.hr (L.Ć.); irena.zmak@fsb.unizg.hr (I.Ž.)

Abstract

Zirconia-based ceramics are widely used in dental applications due to their excellent mechanical and chemical properties. The aim of this study was to evaluate the chemical stability of yttria partially stabilized zirconia (Y-TZP) dental ceramics using a modified testing protocol based on ISO 6872. Two sample groups of Y-TZP material were used: Group 1 - pure polished zirconia, and Group 2 - pure polished zirconia with an additional glaze layer. Chemical stability, defined as corrosion resistance, was assessed by measuring ion release using inductively coupled plasma mass spectrometry (ICP-MS) and by analysing the phase composition using X-ray diffraction (XRD). While ISO 6872 prescribes chemical stability testing in a 4 wt.% aqueous acetic acid (CH_3COOH) solution at 80 °C for 16 hours, the exposure duration in this study was extended to 768 hours (32 days) to enable more accurate determination of long-term corrosion behaviour. Kinetic analysis revealed that degradation followed a near-parabolic rate law, with power-law exponents of n = 2.261 for Group 1 and n = 1.935 for Group 2. The corresponding corrosion rate constants were 3.85×10^{-5} $\mu g^{n} \cdot cm^{-2n} \cdot h^{-1}$ for Sample 1 and 132.3 $\mu g^{n} \cdot cm^{-2n} \cdot h^{-1}$ for Sample 2. XRD results indicated that the corrosion process led to a partial phase transformation of zirconia from the tetragonal to the monoclinic phase.

Keywords: Y-TZP ceramics; dental ceramic; chemical stability; corrosion rate constant

1. Introduction

Over the past few decades, zirconia ceramics have gained significant attention as structural and biomedical materials in restorative dentistry due to their excellent mechanical properties, chemical resistance, high fracture toughness, biocompatibility, and favourable aesthetic qualities [1]. The selection of zirconia as a component for dental prosthesis is also driven by its conservative tooth reduction, minimal impact on opposing dentition wear, and reduced risk of veneer chipping [2]. Zirconia is a polycrystalline oxide ceramic that exists in three allotropes: monoclinic (m), tetragonal (t), and cubic (c). It can achieve relatively high fracture toughness values by manipulating the microstructure and inducing phase changes, specifically by transforming tetragonal zirconia into a monoclinic phase [3]. This phase transformation is accompanied by a volumetric increase, which generates compressive stress within the crack region and slows down crack propagation, consequently increasing the material's fracture toughness. This strengthening mechanism, known as transformation toughening, distinguishes zirconia ceramics as significantly tougher than other ceramic materials [4]. At room temperature, zirconia is in the monoclinic phase (m) and remains stable up to 1170 °C. Between 1170 °C and 2370 °C, it transitions to the tetragonal phase (t), and above

 doi:10.20944/preprints202507.1480.v1

2370 °C, it transforms to the cubic phase (c) with a high melting point (~2700 °C). During processing, the tetragonal phase transforms to the monoclinic phase at around 970 °C, and it is known as the martensitic transformation. The analogy between the transformation and toughening mechanisms in transformation-induced plasticity steels and zirconia led zirconia to be colloquially referred to as "ceramic steel" or "steel-like ceramic" [5].

Several factors influence the transformation toughening of zirconia [6–8]. The volume expansion associated with this transformation is approximately 3-5%, which leads to the formation of cracks and consequently flaws in sintered ceramics [9]. To overcome these drawbacks, various stabilizing oxides, such as Y_2O_3, CeO_2, CaO, MgO, Yb_2O_3, La_2O_3, etc., are incorporated to retain the tetragonal or cubic phases at ambient conditions. Yttria (Y_2O_3) stabilizes the zirconia crystal structure, allowing it to maintain its desirable tetragonal or cubic phases at room temperature. The addition of yttria can resolve problems such as the lack of translucency in zirconia, which presents an inherent drawback due to light scattering at grain boundaries, residual pores, and secondary phases.

3 mol% yttria-stabilized tetragonal zirconia polycrystalline (3Y-TZP) represents the first generation of YSZ (yttria-stabilized zirconia) ceramics commonly used for fixed dental prosthesis frameworks [10,11]. It is typically slightly white and opaque, and can reach full densification with a fine-grained microstructure, offering high wear resistance, fracture toughness, and exceptional bending strength [12–14].

The second generation is also stabilized with 3 mol% yttria but with a small amount of alumina (Al_2O_3) particles in its composition that act as a light scatterer, thus giving the ceramics high translucency. Alumina as a sintering aid greatly enhances powder densification and lowers the sintering temperature [15]. However, the second-generation YSZ is susceptible to low-temperature degradation (LTD), also known as hydrothermal aging, when exposed to aqueous medium at human body temperature. The oxygen vacancies generated when Y^{3+} replaces Zr^{4+} within the cationic sublattice can be replenished by hydroxyl groups in the presence of water, which may potentially contribute to the aging process. During the LTD process, the tetragonal to monoclinic (t→m) transformation of zirconia grains occurs spontaneously, without the application of any external stress, resulting in a volume expansion of 3–4%. The volume expansion leads to the formation of microcracks and potential grain pull-outs [16]. Additionally, it induces surface roughening and degradation of mechanical strength, which may adversely affect dental prostheses [1,17,18]. These microcracks are commonly referred to as corrosion or chemical degradation and are influenced by various pH levels present in the oral environment.

Additionally, physical agents exert their effects through mechanical stress (including both physiological and pathological muscle function), temperature variations (such as consuming hot and cold food or beverages), or during surface treatments of fixed partial dentures (FPD) [17,19]. The material's predisposition to LTD is influenced by various factors, including the level of densification (particularly the porosity), the content and type of stabilizer, grain size, processing properties, and the existence of residual stresses [20,21]. Many contact testing tools are available for monitoring fracture and deformation modes that indicate the degradation of dental ceramics, including sharp-tip micro- and nano-indentations and tests with blunt sphere indenters on flat specimens [22].

Zirconia doped with ceria (CeO_2), or ceria-stabilized tetragonal zirconia polycrystal (Ce-TZP), is considered a promising candidate due to its high hydrothermal stability and fracture toughness in addressing the LTD [23].

The increase in yttria content from 3 mol% to 5 mol% enables the formation of a two-phase mixture (cubic + tetragonal). Cubic crystals possess a greater volume compared to tetragonal crystals, resulting in improved light transmission within the material's structure and enhanced optical properties [24,25]. 8 mol% yttria-stabilized cubic zirconia is transparent and possesses a refractive index of approximately 2.2, which is regarded as high (> 2) within the visible spectrum in optical applications [26]. This structure of zirconia presents the third-generation YSZ and exhibits optical isotropy, reducing the impact of light scattering at grain boundaries. Furthermore, it exhibits a degree of translucency sufficient to replicate the optical characteristics of natural enamel [27–29]. It was, however, also observed that high-translucent zirconia, compared to traditional zirconia, demonstrates a substantial decrease in mechanical performance properties [30–32]. To address this issue, new studies on nanosized zirconia with 1.5 mol% yttria demonstrate excellent mechanical performance while maintaining favourable opacity and good aging resistance [33,34].

Compared to the third generation, the fourth generation 4 mol% yttria-stabilized tetragonal zirconia (4Y-TZP) offers improved mechanical properties, better resistance to aging, wear resistance similar to enamel, and slightly reduced translucency [35].

Recent investigations into the ternary rare earth co-stable zirconia ceramic (1.5Y5.5Ce0.3La-ZrO_2) have demonstrated its capacity to enhance fracture toughness and durability relative to 3Y-TZP substantially. Additionally, biosafety assessments have confirmed that this material is devoid of cytotoxic effects [36].

Another advantage of dental zirconia ceramics is their ability to be processed in various ways by computer-aided design and manufacturing (CAD/CAM) technology [37,38]. Moreover, CAD/CAM technology allows shaping this material from pre-sintered blocks through soft machining and sintering at approximately 1450 °C [39]. This allows for enhancing its usability for solid core structures (bridge construction) or monolithic dental crowns [19,20,40]. Dental abutments and implants can also be made from zirconia using such advanced manufacturing technologies [41,42]. CAD/CAM methods have recently been used in studies to produce multilayer monolithic zirconia with polychromatic layers that mimic natural tooth colour gradients, thereby providing good aesthetics while also enabling efficient fabrication and excellent functionality [43]. It was shown that a uniform grain size, despite having different amounts of t-ZrO_2 and c-ZrO_2 phases due to varying compositions, positively affects the flexural strength of multilayer Y-TZP ceramics [44].

Artificial intelligence (AI) is also used to assist in computer-aided design and manufacturing of zirconia restorations, since AI algorithms help automate repetitive designing tasks, lower human errors, and improve manufacturing efficiency and accuracy [45,46]. Currently, there is a need to enhance education and training in the field of AI among dentistry professionals [47].

Additive manufacturing (AM) has become a well-established technique in dentistry, especially with polymers and metals. Although AM allows for direct dental implant shaping with distinctive geometries and specified topography, AM of zirconia ceramic still faces challenges [48–50]. These include developing suitable ceramic printers, preparing ceramic raw materials, and controlling process parameters, among other issues, as dental objects require precise tolerances and consistent, reliable mechanical properties [51,52]. The 3D printing of ceramics constitutes a promising technique within the field of dentistry, as it obviates the need for traditional, high-cost molds. Moreover, components can be designed with complex shapes, intricate details, and high precision [53].

The most prevalent method of additive manufacturing for biomedical implants is vat photopolymerization (VPP) [54]. A ceramic slurry is prepared by mixing ceramic powder with photopolymer resin, i.e., light-sensitive polymer that hardens when exposed to ultraviolet (UV) light, dispersants, and binders. Vat photopolymerization of ceramics involves layer-by-layer UV curing of the resin to form a green body, which is then debinded to remove the polymer, and sintered. Dental zirconia milled using computer numerical control (CNC) machining has greater flexural strength and fatigue resistance than when processed by VPP, but fracture toughness and hardness are similar [55]. A challenge in the fabrication of ceramic dental prostheses utilizing VPP pertains to the employment of slurries composed of organic monomers, which additionally raise environmental concerns. Consequently, new aqueous zirconia suspensions are being investigated [56].

Research on manufacturing processes emphasizes innovative sintering techniques, such as speeding up the process to meet the rising demand for same-day dental prosthetic production. High-speed sintering employs cooling rates of 120 $°C \cdot min^{-1}$ or more, compared to the typical 10 $°C \cdot min^{-1}$. The disadvantages of this approach include reduced translucency of 3Y-TZP, caused by a decrease in yttria-rich tetragonal phase with low tetragonality, and an increase in yttria-lean tetragonal phase with high tetragonality [57]. High-speed sintering also diminishes the mechanical properties of 3Y-TZP; however, they remain sufficiently acceptable for clinical use [58].

 doi:10.20944/preprints202507.1480.v1

The primary challenge associated with monolithic ceramics lies in the finishing techniques employed, namely glazing and high polishing. Glazing is a conventional method used to apply a glassy layer on the outer surface of ceramic restorations (veneers or crowns). This glassy layer forms during sintering due to viscous flow, which occurs when the glass component fuses at high temperatures. Glazing provides several benefits, including reducing porosity, minimizing existing flaws, thereby improving surface texture, and consequently enhancing the mechanical strength of dental ceramics. Dental ceramic glazes typically consist of silica, porcelain, glass-ceramics, or dense crystalline solids [19,59]. Novel surface modification processes include atomic layer deposition (ALD) for coating of zirconia dental implants, where, for example, the deposition of titania (TiO_2) and alumina has proven to be chemically stable and highly biocompatible [60,61].

The translucency and colour stability, which are important for long-term aesthetics, of zirconia restorations are influenced by changes in oral temperature, pH levels, and mechanical stresses [62]. The surface roughness of dental ceramics causes the wear of opposing enamel to increase, as well as plaque formation, discoloration, and staining. The surface roughness of dental ceramics can be minimized through various polishing methods, thereby prolonging their lifespan [63,64].

Corrosion of dental ceramics is associated with degradation that occurs in the oral cavity due to various chemical or mechanical influences. Dental materials are exposed to a range of pH values in the oral cavity, varying from highly acidic (due to gastric reflux) to slightly basic (resulting from the ingestion of various liquids and foods). The temperature also varies depending on whether hot or cold liquids are ingested [20,65]. Therefore, it is of high importance to assess the chemical stability of dental ceramics in various corrosive environments to produce long-lasting and stable dental applications.

Given these considerations, it is essential to systematically investigate the chemical stability and degradation kinetics of different zirconia surfaces under prolonged exposure. In this study, the long-term corrosion behaviour of Y-TZP dental ceramics was evaluated using an extended ISO 6872 protocol. In this work, two types of specimens were tested: polished unglazed Y-TZP and polished Y-TZP with an additional glazed layer. Chemical degradation was assessed by ion release analysis using high-resolution ICP-MS and phase analysis by XRD. The results were interpreted using kinetic models to quantify corrosion rates and compare the durability of glazed vs. non-glazed surfaces of Y-TZP dental ceramics.

2. Materials and Methods

2.1. Characterization of Yttria Partially Stabilized Zirconia (Y-TZP) Dental Ceramics

For this research, two groups of Y-TZP dental ceramic samples (n = 10 per group), stabilized with 4.1 wt.% Y_2O_3 were prepared. The first group (Sample 1) consisted of sintered, polished, and non-glazed specimens. The second group (Sample 2) comprised sintered, polished specimens that were fully glazed on all surfaces to simulate the finishing process used in the fabrication of monolithic crowns. Samples of Y-TZP dental ceramics (non-glazed and glazed) were provided by BruxZir, Glidewell Laboratories (Newport Beach, CA, USA). The manufacturer provided samples in the shape of square plates, 10 × 10 × 2 mm, sintered using the usual sintering regime employed in the production of ceramic restorations at Glidewell Laboratories. The glaze was standard, feldspathic. The declared chemical composition of the Y-TZP dental ceramics is shown in Table 1.

Table 1. Chemical composition of the Y-TZP dental ceramics expressed as weight percent (wt.%).

Element	Y_2O_3	HfO_2	Al_2O_3	SiO_2	Fe_2O_3	Na_2O	ZrO_2
wt.%	4.1	4.0	0.34	<0.01	<0.01	<0.01	balance

The phase composition of Y-TZP dental ceramics was determined by powder X-ray diffraction, PXRD (Shimadzu XRD6000, Shimadzu Corporation, Kyoto, Japan) with CuKα radiation. A step size

 doi:10.20944/preprints202507.1480.v1

of 0.02 degrees between 10° and 80° 2θ, and a counting time of 0.6 s, were used under an accelerating voltage of 40 kV and a current of 30 mA.

The morphology of the prepared sintered samples was analysed using a scanning electron microscope (SEM) (Tescan Vega TS5136LS, Prague, Czech Republic). Before the SEM analysis, the polished sample of Y-TZP dental ceramic was thermally etched at 1480 °C, for 12 min, according to the ASTM Standard E112-96.

2.2. Monitoring of the Chemical Stability of the Y-TZP Dental Ceramics

Samples groups of Y-TZP dental ceramics, Sample group 1 (non-glazed) and Sample group 2 (glazed), with dimensions of 10 × 10 × 2 mm, were washed in distilled water in an ultrasonic bath (1510 DTH, Electron Microscopy Sciences, Hatfield, PA, USA) to remove any contaminants. The samples were then dried at 150 °C. Before the cleaning of the samples, their dimensions were verified using a digital calliper (Mitutoyo, Aurora, IL, USA). The mass of each sample was measured using an analytical balance (Ohaus Analytical Plus) to an accuracy of $\pm 10^{-5}$ g, and the surface area was subsequently calculated. Each sample was immersed in 10 mL of 4 wt.% aqueous CH_3COOH solution in individual polypropylene (PP) tubes, ensuring complete immersion in the corrosive medium. To prevent local enrichment of eluted components at the sample surface, the tubes were sealed and placed in a thermostatic shaker (Innova 4080 Incubator-Shaker, Herisau, Switzerland), operating at 80 °C and 200 rpm.

The corrosion tests were conducted at a temperature of 80 °C for 16 hours to 32 days (768 hours). The sample surface area / 4 wt.% CH_3COOH solution volume ratio was 0.248 $cm^2 \cdot mL^{-1}$. Parallel with the corrosion testing, a blind test was also performed. The measurements were conducted after 16 hours, 8 days (192 hours), 16 days (384 hours), and 32 days (768 hours) of immersion. After the designated exposure periods, samples were removed, rinsed with distilled water, dried in an oven at 150 °C, and weighed. For each exposure condition, ten replicates were tested simultaneously ($n = 10$).

The concentrations of Al^{3+}, Na^{+}, Ca^{2+}, K^{+}, Si^{4+}, Fe^{3+}, Zn^{2+}, Mg^{2+}, Sr^{2+}, Ba^{2+}, Y^{3+}, and Zr^{4+} ions released into the corrosive solution were determined using high-resolution inductively coupled plasma mass spectrometry (HR-ICP-MS; Thermo Fisher Scientific, Waltham, MA, USA). The results are reported as the amount of ions (M^{n+}) released per unit surface area of the tested Y-TZP dental ceramic samples. After the time had elapsed, the samples were washed with distilled water in an ultrasonic bath (ISO 3696), dried, and weighed.

3. Results

3.1. Structural and Morphological Characterization of Yttria Partially Stabilized Zirconia (Y-TZP) Dental Ceramics

To investigate the correlation between the corrosion process and phase transformations in Y-TZP dental ceramics, samples were analysed by X-ray diffraction (XRD) before and after exposure to the corrosive medium (Figure 1). The XRD results revealed that the untreated Y-TZP ceramics (before corrosion, Y-TZP b.c.) contained only the tetragonal ZrO_2 phase (ICDD 20-1089). In the samples exposed to 4 wt.% CH_3COOH at 80 °C (after corrosion, Y-TZP a.c.), the tetragonal ZrO_2 phase (t-ZrO_2) remained the dominant crystalline phase. However, a small amount of monoclinic ZrO_2 (m-ZrO_2) (ICDD 37-1484) was also detected. These findings indicate that partial transformation from the tetragonal to the monoclinic phase of ZrO_2 occurred during the corrosion process, which is in agreement with previously reported literature [66,67].

 doi:10.20944/preprints202507.1480.v1

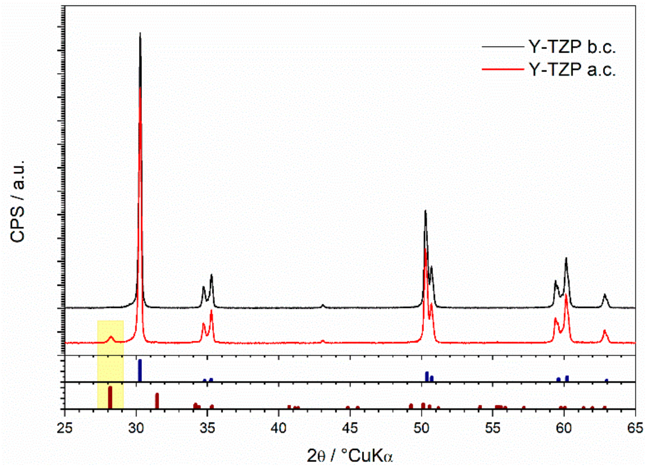

Figure 1. Comparison of diffraction patterns of the Y-TZP dental ceramics before (Y-TZP b.c.) and after (Y-TZP a.c.) corrosion test.

Figure 2 shows the SEM micrograph of the polished and thermally etched surface of Y-TZP dental ceramics (Sample 1). The average grain size, determined according to ASTM Standard E112–96 (2004), is 425±137 nm.

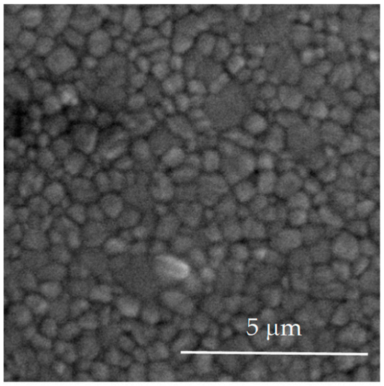

Figure 2. Polished and thermally etched surface images of the Y-TZP dental ceramics (thermal etching at 1480 °C, 12 min).

3.2. Amount of Ions Released in Corrosive Solution from Yttria Partially Stabilized Zirconia (Y-TZP) Dental Ceramics

Figure 3 shows the relationship between the amount of eluted Y^{4+} and Zr^{4+} ions from non-glazed Y-TZP dental ceramics (Sample 1) and the time of immersion in the 4 wt.% CH_3COOH solution at 80 °C.

doi:10.20944/preprints202507.1480.v1

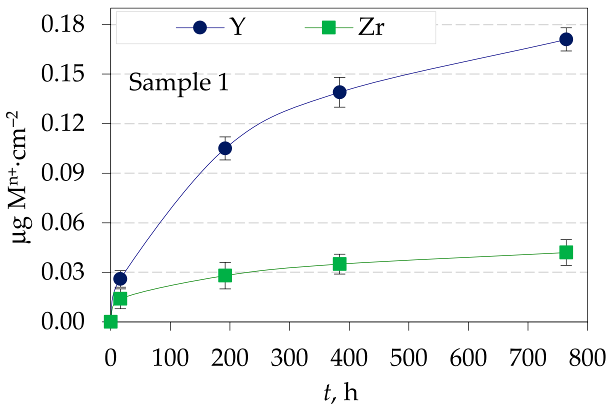

Figure 3. Amount of eluted Y^{4+} and Zr^{4+} ions from non-glazed Y-TZP dental ceramics (Sample 1) in 4 wt.% CH_3COOH solution as a function of immersion time at 80 °C (mean value and standard deviation).

Figure 4 shows the relationship between the amount of eluted Al^{3+}, Na^{+}, Ca^{2+}, K^{+}, Si^{4+} (Figure 4a), Fe^{3+}, Zn^{2+}, Mg^{2+} (Figure 4b), Sr^{2+}, Ba^{2+}, Y^{3+} and Zr^{4+} ions (Figure 4c) from Y-TZP dental ceramics Sample 2 (sintered, polished and glazed) and the time of immersion in the 4 wt.% CH_3COOH solution at 80 °C.

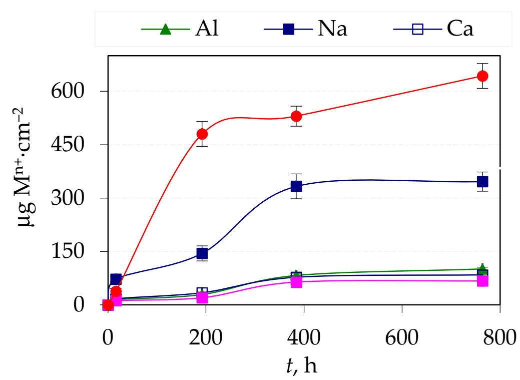

(**a**)

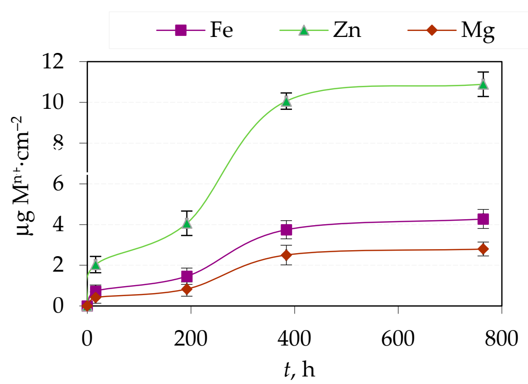

(**b**)

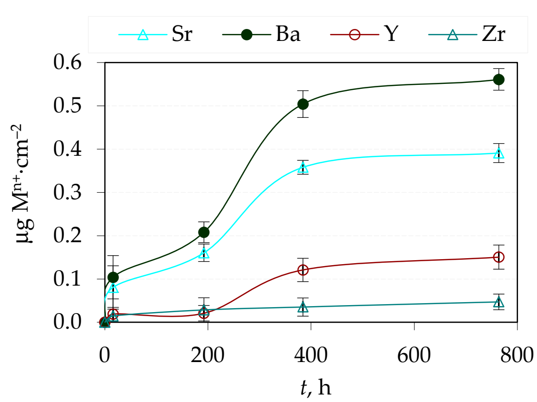

(**c**)

 doi:10.20944/preprints202507.1480.v1

Figure 4. The amount of eluted (**a**) Al^{3+}, Na^{+}, Ca^{2+}, K^{+}, Si^{4+}; (**b**) Fe^{3+}, Zn^{2+}, Mg^{2+}; (**c**) Sr^{2+}, Ba^{2+}, Y^{3+} and Zr^{4+} ions from Y-TZP dental ceramics Sample 2 in the 4 wt.% CH_3COOH solution as a function of immersion time at 80 °C (mean value and standard deviation).

Both zirconia samples exhibited minimal Zr^{4+} and Y^{3+} ion release, indicating excellent chemical stability of the testing ceramic samples under the tested conditions (Figures 3 and 4c). The total amount of eluted ions from Y-TZP dental ceramics (Sample 1 and Sample 2) after immersion in 4 wt.% CH_3COOH solution as a function of immersion time at 80 °C is presented in Figures 5a and 5b. The overall ion release represents the cumulative sum of all individual ions leached from the Y-TZP ceramics into the acetic acid solution throughout the experiment. In general, the corrosion susceptibility—expressed as the total amount of eluted ions—increased with immersion time for both Y-TZP samples. A higher cumulative ion release was observed for Sample 2, which included a glaze layer. These findings suggest that Sample 2, which contains a glaze layer with a glassy or amorphous structure, is more susceptible to corrosion, most likely due to congruent dissolution.

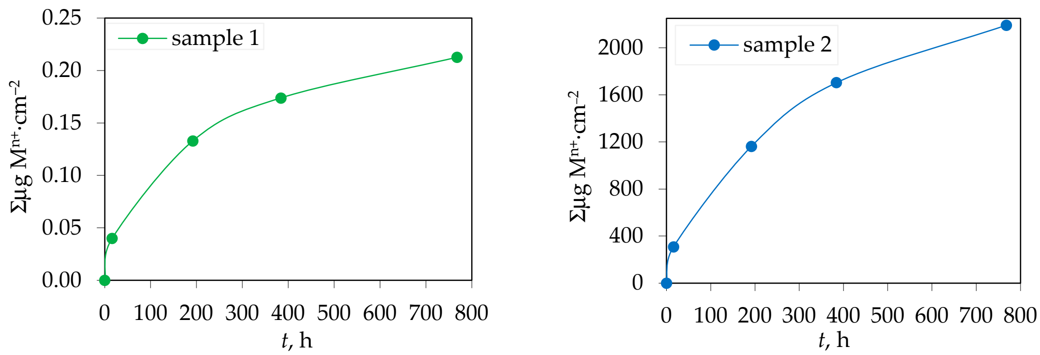

(**a**) (**b**)

Figure 5. Total overall amount of eluted ions from Y-TZP dental ceramics: (**a**) Sample 1; (**b**) Sample 2 after immersion in the 4 wt.% CH_3COOH solution as a function of immersion time at 80 °C.

3.3. Corrosion Rate of Yttria Partially Stabilized Zirconia (Y-TZP) Dental Ceramics in CH_3COOH

In the present study, the measurement of eluted ions was used to investigate the corrosion kinetics. The variation of corrosion rate over time may follow linear, parabolic, logarithmic, or other rate laws. The following equation was applied to determine which rate law best describes the experimental data:

$$\left(\sum \frac{m(\mathrm{M}^{\mathrm{n}+})}{A}\right)^{n} = K_{\mathrm{p}} \cdot t \quad (1)$$

where $\Sigma m\ (\mathrm{M}^{\mathrm{n}+})$ stands for mass of overall amount of eluted ions (Al^{3+}, Ca^{2+}, Fe^{3+}, Mg^{2+}, Na^{+}), μg; A for specific surface, cm^2; n for the power exponent; K_p for corrosion rate constant, $\mu g^{n}\cdot cm^{-2n}\cdot h^{-1}$; and t for time of the ceramic exposure to the corrosive media, h.

The power exponent n was determined from the linear plot of ln (Σμg ($M^{n+}\cdot cm^{-2}$) versus ln t (Figures 6a and 6b), with n calculated from the slope of the line. The corrosion rate constants K_p were obtained from the slope of the linear plot of $(\Sigma\mu g(M^{n+}\cdot cm^{-2})^{n}$ versus t (Figure 6c and 6d). The calculated values of the power exponent (n), the corrosion rate constants (K_p, $\mu g^{n}\cdot cm^{-2n}\cdot h^{-1}$), and corresponding correlation coefficients (R^2) are summarized in Table 2.

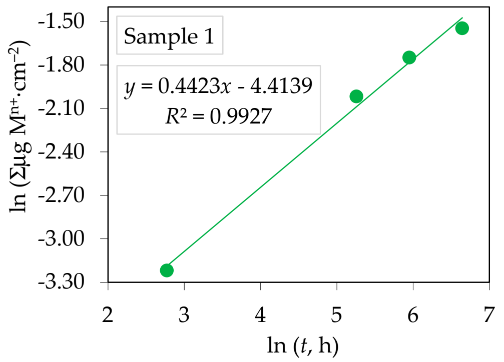

(**a**)

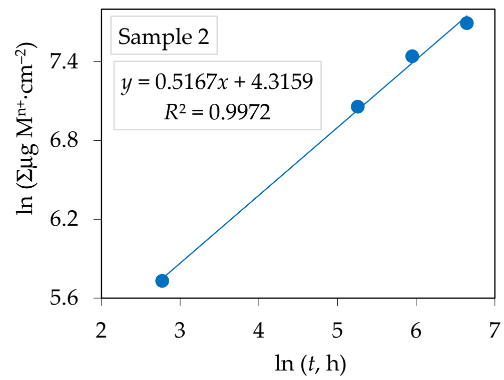

(**b**)

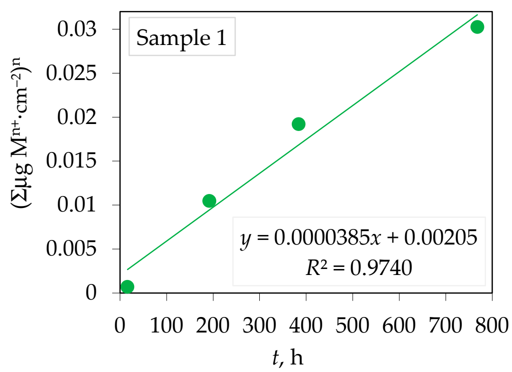

(**c**)

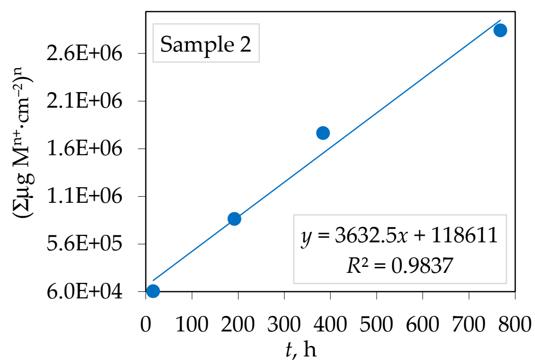

(**d**)

Figure 6. Determination of the power exponent n for: (**a**) Sample 1; (**b**) Sample 2; Determination of the corrosion rate constants for: (**c**) Sample 1; (**d**) Sample 2 of Y-TZP dental ceramics in the 4 wt.% CH_3COOH solution at 80 °C.

The power exponent (*n*) was 2.261 and 1.935 for Sample 1 and Sample 2, respectively, which means that the corrosion kinetics of Y-TZP ceramics in the 4 wt.% CH_3COOH aqueous solution at 80 °C follows the near-parabolic law.

Table 2. Values of the parabolic corrosion rate constant (K_P) for Sample 1 (non-glazed Y-TZP) and for Sample 2 (glazed Y-TZP).

Y-TZP	*n*	R^2	K_P, μg^n·cm^{-2n}·h^{-1}	R^2
Sample 1	2.261±0.004	0.9927	$3.85 \times 10^{-5} \pm 4.45 \times 10^{-6}$	0.9740
Sample2	1.935±0.015	0.9972	3632.5±330.7	0.9837

The corrosion rate constant for Sample 2 (glazed Y-TZP) is 3632.5 μg^n·cm^{-2n}·h^{-1} and represents a significantly higher value of the corrosion rate constant compared to the dental ceramic sample without glaze (3.85×10^{-5} μg^n·cm^{-2n}·h^{-1}, Sample 1).

4. Conclusions

The chemical stability of polycrystalline yttria partially stabilized zirconia (Y-TZP) ceramics was tested in a 4 wt.% CH_3COOH aqueous solution (pH=2.49) at a temperature of 80 °C for 16 hours, 192 hours (8 days), 384 hours (16 days), and 768 hours (32 days). X-ray diffraction analysis (XRD) before corrosion revealed the presence of only one crystalline phase in the Y-TZP sample: tetragonal. The

 doi:10.20944/preprints202507.1480.v1

average grain size of Y-TZP crystals was 425±137 nm. XRD revealed a partial phase transformation from tetragonal to monoclinic zirconia occurred during the corrosion process.

In the extracted eluates after the specified time intervals, the quantities of the following ions were measured: Si^{4+}, Na^{+}, Al^{3+}, Ca^{2+}, K^{+}, Zn^{2+}, Fe^{3+}, Mg^{2+}, Ba^{2+}, Sr^{2+}, Y^{3+}, and Zr^{4+}.

For Sample 1 (uncoated polished Y-TZP), the leaching of Y^{3+} and Zr^{4+} ions were detected. Y^{3+} exhibited higher leaching compared to Zr^{4+}.

For Sample 2 (Y-TZP with glaze coating), the leaching of the following ions was detected: Si^{4+}, Na^{+}, Al^{3+}, Ca^{2+}, K^{+}, Zn^{2+}, Fe^{3+}, Mg^{2+}, Ba^{2+}, Sr^{2+}, Y^{3+}, and Zr^{4+}. Si^{4+} exhibited the highest release, while Zr^{4+} was leached in the smallest amount. After 768 hours (32 days) of exposure, the ion release from Sample 2 decreased in the following order: $Si^{4+} > Na^{+} > Al^{3+} > Ca^{2+} > K^{+} > Zn^{2+} > Fe^{3+} > Mg^{2+} > Ba^{2+} > Sr^{2+} > Y^{3+} > Zr^{4+}$.

The dominant mechanism driving the corrosion and ion release appears to be congruent dissolution with simple dissociation. Based on the results, it can be concluded that the glaze layer, due to its amorphous or glassy nature, is significantly more susceptible to corrosion. The mechanism of the corrosion, however, remained unchanged. In contrast, the uncoated Y-TZP dental ceramics demonstrated excellent chemical stability, with very low ion release even after 768 hours of exposure to 4 wt.% acetic acid at 80 °C.

Author Contributions: Conceptualization, L.Ć., S.Š. and I.Ž.; methodology, L.Ć., S.Š. and I.Ž; formal analysis, S.Š., V.M., and L.Ć.; investigation, S.Š., and L.Ć.; data curation, S.Š., V.M., I.Ž. and L.Ć.; writing—original draft preparation, L.Ć., S.Š. I.G. and I.Ž.; writing—review and editing, L.Ć., S.Š. I.G., V.M., I.Ž., and K.M.; visualization, L.Ć. and I.Ž.; supervision, L.Ć. and K.M.; project administration, L.Ć.; funding acquisition, L.Ć. All authors have read and agreed to the published version of the manuscript.

Data Availability Statement: Data will be made available upon reasonable request.

Acknowledgements: We thank Josef Rothaut from BruxZir, Glidewell Laboratories, for providing dental ceramics samples.

Conflicts of Interest: The authors declare no conflicts of interest.

Abbreviations

The following abbreviations are used in this manuscript:

3Y-TZP	3 mol% yttria-stabilized tetragonal zirconia polycrystal
4Y-TZP	4 mol% yttria-stabilized tetragonal zirconia polycrystal
AI	Artificial intelligence
ALD	Atomic layer deposition
c	Cubic phase
CAD/CAM	Computer-aided design and computer-aided manufacturing
Ce-TZP	Ceria-stabilized tetragonal zirconia polycrystal
CNC	Computer numerical control machining
FPD	Fixed partial denture
HR-ICP-MS	High-resolution inductively coupled plasma mass spectrometry
ICP-MS	Inductively coupled plasma mass spectrometry
LTD	Low-temperature degradation
m	Monoclinic phase
SEM	Scanning electron microscope
t	Tetragonal phase
VPP	Vat photopolymerization
XRD	X-ray diffraction
YSZ	Yttria-stabilized zirconia polycrystal
Y-TZP	Yttria partially stabilized zirconia polycrystal

References

1. Han, J.; Zhang, F.; Van Meerbeek, B.; Vleugels, J.; Braem, A.; Castagne, S. Laser Surface Texturing of Zirconia-Based Ceramics for Dental Applications: A Review. *Materials Science and Engineering: C* **2021**, *123*, 112034, doi:10.1016/j.msec.2021.112034.
2. Mohammed, M.S.; Mohsen, C.A. Effect of Corrosion On Some Properties of Dental Ceramics. *Sys Rev Pharm* **2021**, *12*, 584–588.
3. Lughi, V.; Sergo, V. Low Temperature Degradation -Aging- of Zirconia: A Critical Review of the Relevant Aspects in Dentistry. *Dental Materials* **2010**, *26*, 807–820, doi:10.1016/j.dental.2010.04.006.
4. Ćorić, D.; Majić Renjo, M.; Žmak, I. Critical Evaluation of Indentation Fracture Toughness Measurements with Vickers Indenter on Yttria-Stabilized Zirconia Dental Ceramics: Kritische Bewertung Der Mittels Vickers-Indentierung Ermittelten Bruchzähigkeit von Mit Yttriumoxid Stabilisierten Tetragonalen Zirkonoxid-Dentalkeram. *Mat.-wiss. u. Werkstofftech.* **2017**, *48*, 767–772, doi:10.1002/mawe.201700026.
5. Ceramic Steel? In *Sintering Key Papers*; Springer Netherlands: Dordrecht, 1990; pp. 253–257 ISBN 978-94-010-6818-5.
6. Elshazly, E.S.; El-Hout, S.M.; Ali, M.E.-S. Yttria Tetragonal Zirconia Biomaterials: Kinetic Investigation. *Journal of Materials Science & Technology* **2011**, *27*, 332–337, doi:10.1016/s1005-0302(11)60070-4.
7. Bohé, A.E.; Gamboa, J.J.A.; Pasquevich, D.M. Enhancement of the Martensitic Transformation of Tetragonal Zirconia Powder in the Presence of Iron Oxide. *Materials Science and Engineering: A* **1999**, *273–275*, 218–221, doi:10.1016/s0921-5093(99)00374-3.
8. Wongkamhaeng, K.; Dawson, D.V.; Holloway, J.A.; Denry, I. Effect of Surface Modification on In-Depth Transformations and Flexural Strength of Zirconia Ceramics. *Journal of Prosthodontics* **2019**, *28*, doi:10.1111/jopr.12908.
9. Majić Renjo, M.; Ćurković, L.; Štefančić, S.; Ćorić, D. Indentation Size Effect of Y-TZP Dental Ceramics. *Dental Materials* **2014**, *30*, e371–e376, doi:10.1016/j.dental.2014.08.367.
10. Singh, R.G.; Lyons, K.M.; Waddell, J.N.; Li, K.C. Effect of Thermocycling on the Mechanical Properties, Inorganic Particle Release and Low Temperature Degradation of Glazed High Translucent Monolithic 3Y-TZP Dental Restorations. *Journal of the Mechanical Behavior of Biomedical Materials* **2022**, *136*, 105495, doi:10.1016/j.jmbbm.2022.105495.
11. El Yamani, A.; Soualhi, H.; Alaoui, Y.A. The Evolution of Dental Zirconia: Advancements and Applications. *CODS - Journal of Dentistry* **2025**, *16*, 20–27, doi:10.5005/jp-journals-10063-0164.
12. Toksoy, D.; Önöral, Ö. Optical Behavior of Zirconia Generations. *cjms* **2024**, *9*, 380–389, doi:10.4274/cjms.2024.2024-29.
13. Zhang, F.; Inokoshi, M.; Batuk, M.; Hadermann, J.; Naert, I.; Van Meerbeek, B.; Vleugels, J. Strength, Toughness and Aging Stability of Highly-Translucent Y-TZP Ceramics for Dental Restorations. *Dental Materials* **2016**, *32*, e327–e337, doi:10.1016/j.dental.2016.09.025.
14. Jitwirachot, K.; Rungsiyakull, P.; Holloway, J.A.; Jia-mahasap, W. Wear Behavior of Different Generations of Zirconia: Present Literature. *International Journal of Dentistry* **2022**, *2022*, 1–17, doi:10.1155/2022/9341616.
15. Huang, W.; Zhou, J.; Ren, C.; Zhang, F.; Tang, J.; Omran, M.; Chen, G. Sintering Behaviour and Properties of Zirconia Ceramics Prepared by Pressureless Sintering. *Ceramics International* **2023**, *49*, 27192–27200, doi:10.1016/j.ceramint.2023.05.267.
16. Johansson, C.; Franco Tabares, S.; Larsson, C.; Papia, E. Laboratory, Clinical-Related Processing and Time-Related Factors' Effect on Properties of High Translucent Zirconium Dioxide Ceramics Intended for Monolithic Restorations A Systematic Review. *Ceramics* **2023**, *6*, 734–797, doi:10.3390/ceramics6010045.
17. Magnani, G.; Fabbri, P.; Leoni, E.; Salernitano, E.; Mazzanti, F. New Perspectives on Zirconia Composites as Biomaterials. *J. Compos. Sci.* **2021**, *5*, 244, doi:10.3390/jcs5090244.
18. Sheng, Y.; Wang, L.; Dou, R.; Zhu, F.; Gao, Y. Effects of Dopants with Varying Cationic Radii on the Mechanical Properties and Hydrothermal Aging Stability of Dental 3Y-TZP Ceramics Fabricated via Vat Photopolymerization. *Ceramics International* **2025**, *51*, 11857–11870, doi:10.1016/j.ceramint.2025.01.038.
19. Štefančić, S.; Ćurković, L.; Baršić, G.; Majić-Renjo, M.; Mehulić, K. Investigation of Glazed Y-TZP Dental Ceramics Corrosion by Surface Roughness Measurement. *Acta Stomatol Croat* **2013**, *47*, 163–168, doi:10.15644/asc47/2/8.

20. Nowicka, A.; El-Maghraby, H.F.; Švančárková, A.; Galusková, D.; Reveron, H.; Gremillard, L.; Chevalier, J.; Galusek, D. Corrosion and Low Temperature Degradation of 3Y-TZP Dental Ceramics under Acidic Conditions. *Journal of the European Ceramic Society* **2020**, *40*, 6114–6122, doi:10.1016/j.jeurceramsoc.2020.06.019.
21. Toma, F.R.; Porojan, S.D.; Vasiliu, R.D.; Porojan, L. The Effect of Polishing, Glazing, and Aging on Optical Characteristics of Multi-Layered Dental Zirconia with Different Degrees of Translucency. *JFB* **2023**, *14*, 68, doi:10.3390/jfb14020068.
22. Zhang, Y.; Lawn, B.R. Evaluating Dental Zirconia. *Dental Materials* **2019**, *35*, 15–23, doi:10.1016/j.dental.2018.08.291.
23. Cailliet, S.; Roumanie, M.; Croutxé-Barghorn, C.; Bernard-Granger, G.; Laucournet, R. Y-TZP, Ce-TZP and as-Synthesized Ce-TZP/Al_2O_3 Materials in the Development of High Loading Rate Digital Light Processing Formulations. *Ceramics International* **2021**, *47*, 3892–3900, doi:10.1016/j.ceramint.2020.09.251.
24. Da Rosa, L.S.; Pilecco, R.O.; Sarkis-Onofre, R.; Kantorski, K.Z.; Valandro, L.F.; Rocha Pereira, G.K. Should Finishing, Polishing or Glazing Be Performed after Grinding YSZ Ceramics? A Systematic Review and Meta-Analysis. *Journal of the Mechanical Behavior of Biomedical Materials* **2023**, *138*, 105654, doi:10.1016/j.jmbbm.2023.105654.
25. Alqutaibi, A.Y.; Ghulam, O.; Krsoum, M.; Binmahmoud, S.; Taher, H.; Elmalky, W.; Zafar, M.S. Revolution of Current Dental Zirconia: A Comprehensive Review. *Molecules* **2022**, *27*, 1699, doi:10.3390/molecules27051699.
26. Chen, P.; Li, X.; Tian, F.; Liu, Z.; Hu, D.; Xie, T.; Liu, Q.; Li, J. Fabrication, Microstructure, and Properties of 8 Mol% Yttria-Stabilized Zirconia (8YSZ) Transparent Ceramics. *J Adv Ceram* **2022**, *11*, 1153–1162, doi:10.1007/s40145-022-0602-6.
27. Kim, H.-K. Effect of A Rapid-Cooling Protocol on the Optical and Mechanical Properties of Dental Monolithic Zirconia Containing 3–5 Mol% Y2O3. *Materials* **2020**, *13*, 1923, doi:10.3390/ma13081923.
28. Kui, A.; Manziuc, M.; Petruțiu, A.; Buduru, S.; Labuneț, A.; Negucioiu, M.; Chisnoiu, A. Translucent Zirconia in Fixed Prosthodontics—An Integrative Overview. *Biomedicines* **2023**, *11*, 3116, doi:10.3390/biomedicines11123116.
29. Alrabeah, G.; Al-Sowygh, A.H.; Almarshedy, S. Use of Ultra-Translucent Monolithic Zirconia as Esthetic Dental Restorative Material: A Narrative Review. *Ceramics* **2024**, *7*, 264–275, doi:10.3390/ceramics7010017.
30. Han, M.-K. Advances and Challenges in Zirconia-Based Materials for Dental Applications. *J. Korean Ceram. Soc.* **2024**, *61*, 783–799, doi:10.1007/s43207-024-00416-7.
31. Mavriqi, L.; Traini, T. Mechanical Properties of Translucent Zirconia: An In Vitro Study. *Prosthesis* **2023**, *5*, 48–59, doi:10.3390/prosthesis5010004.
32. Hjerppe, J.; Özcan, M. Zirconia: More and More Translucent. *Curr Oral Health Rep* **2023**, *10*, 203–211, doi:10.1007/s40496-023-00344-1.
33. Roitero, E.; Reveron, H.; Gremillard, L.; Garnier, V.; Ritzberger, C.; Chevalier, J. Ultra-Fine Yttria-Stabilized Zirconia for Dental Applications: A Step Forward in the Quest towards Strong, Translucent and Aging Resistant Dental Restorations. *Journal of the European Ceramic Society* **2023**, *43*, 2852–2863, doi:10.1016/j.jeurceramsoc.2022.11.048.
34. Kern, F.; Osswald, B. Mechanical Properties of an Extremely Tough 1.5 Mol% Yttria-Stabilized Zirconia Material. *Ceramics* **2024**, *7*, 1066–1084, doi:10.3390/ceramics7030070.
35. Arellano Moncayo, A.M.; Peñate, L.; Arregui, M.; Giner-Tarrida, L.; Cedeño, R. State of the Art of Different Zirconia Materials and Their Indications According to Evidence-Based Clinical Performance: A Narrative Review. *Dentistry Journal* **2023**, *11*, 18, doi:10.3390/dj11010018.
36. Zhong, H.; Liu, Y.; Zhou, Z.; Fan, Z.; Shu, Z.; Wu, L. Preparation and Properties of Ternary Rare Earth Co-Stabilized Zirconia Ceramics for Dental Restorations. *Ceramics International* **2024**, *50*, 799–809, doi:10.1016/j.ceramint.2023.10.164.
37. Jakovac, M.; Klaser, T.; Bafti, A.; Skoko, Ž.; Pavić, L.; Žic, M. The Effect of Y^{3+} Addition on Morphology, Structure, and Electrical Properties of Yttria-Stabilized Tetragonal Zirconia Dental Materials. *Materials* **2022**, *15*, 1800, doi:10.3390/ma15051800.

38. Iliev, G.; Vasileva, R.; Kirov, D.; Deliverska, E.; Kirilova, J. Mechanical Resistance of Different Dental Ceramics and Composite, Milled, or Printed Materials: A Laboratory Study. *Applied Sciences* **2024**, *14*, 11129, doi:10.3390/app142311129.
39. Turon-Vinas, M.; Anglada, M. Strength and Fracture Toughness of Zirconia Dental Ceramics. *Dental Materials* **2018**, *34*, 365–375, doi:10.1016/j.dental.2017.12.007.
40. Oliveira, A.R.; Ziglioli, N.U.; Marocho, S.M.S.; Satterthwaite, J.; Borba, M. Effect of the CAD/CAM Milling Protocol on the Fracture Behavior of Zirconia Monolithic Crowns. *Materials* **2024**, *17*, 2981, doi:10.3390/ma17122981.
41. Lo Giudice, R.; Sindoni, A.; Tribst, J.P.M.; Dal Piva, A.M.D.O.; Lo Giudice, G.; Bellezza, U.; Lo Giudice, G.; Famà, F. Evaluation of Zirconia and High Performance Polymer Abutment Surface Roughness and Stress Concentration for Implant-Supported Fixed Dental Prostheses. *Coatings* **2022**, *12*, 238, doi:10.3390/coatings12020238.
42. Kohal, R.J.; Riesterer, E.; Vach, K.; Patzelt, S.B.M.; Iveković, A.; Einfalt, L.; Kocjan, A.; Hillebrecht, A.-L. Fracture Resistance of a Bone-Level Two-Piece Zirconia Oral Implant System—The Influence of Artificial Loading and Hydrothermal Aging. *JFB* **2024**, *15*, 122, doi:10.3390/jfb15050122.
43. Kang, C.-M.; Peng, T.-Y.; Wu, Y.-A.; Hsieh, C.-F.; Chi, M.-C.; Wu, H.-Y.; Lin, Z.-C. Comparison of Optical Properties and Fracture Loads of Multilayer Monolithic Zirconia Crowns with Different Yttria Levels. *JFB* **2024**, *15*, 228, doi:10.3390/jfb15080228.
44. Labetić, A.; Klaser, T.; Skoko, Ž.; Jakovac, M.; Žic, M. Flexural Strength and Morphological Study of Different Multilayer Zirconia Dental Materials. *Materials* **2024**, *17*, 1143, doi:10.3390/ma17051143.
45. Kong, H.-J.; Kim, Y.-L. Application of Artificial Intelligence in Dental Crown Prosthesis: A Scoping Review. *BMC Oral Health* **2024**, *24*, doi:10.1186/s12903-024-04657-0.
46. Singh, J.; Singh, S.; Verma, A. Artificial Intelligence in Use of ZrO_2 Material in Biomedical Science: Review Paper. *J. Electrochem. Sci. Eng.* **2022**, doi:10.5599/jese.1498.
47. Ivanišević, A.; Tadin, A. Artificial Intelligence and Modern Technology in Dentistry: Attitudes, Knowledge, Use, and Barriers Among Dentists in Croatia—A Survey-Based Study. *Clinics and Practice* **2024**, *14*, 2623–2636, doi:10.3390/clinpract14060207.
48. Zhang, F.; Spies, B.C.; Willems, E.; Inokoshi, M.; Wesemann, C.; Cokic, S.M.; Hache, B.; Kohal, R.J.; Altmann, B.; Vleugels, J.; et al. 3D Printed Zirconia Dental Implants with Integrated Directional Surface Pores Combine Mechanical Strength with Favorable Osteoblast Response. *Acta Biomaterialia* **2022**, *150*, 427–441, doi:10.1016/j.actbio.2022.07.030.
49. Sokola, P.; Ptáček, P.; Bafti, A.; Panžić, I.; Mandić, V.; Blahut, J.; Kalina, M. Comprehensive Study of Stereolithography and Digital Light Processing Printing of Zirconia Photosensitive Suspensions. *Ceramics* **2024**, *7*, 1616–1638, doi:10.3390/ceramics7040104.
50. Dewan, H. Clinical Effectiveness of 3D-Milled and 3D-Printed Zirconia Prosthesis—A Systematic Review and Meta-Analysis. *Biomimetics* **2023**, *8*, 394, doi:10.3390/biomimetics8050394.
51. Nakai, H.; Inokoshi, M.; Nozaki, K.; Komatsu, K.; Kamijo, S.; Liu, H.; Shimizubata, M.; Minakuchi, S.; Van Meerbeek, B.; Vleugels, J.; et al. Additively Manufactured Zirconia for Dental Applications. *Materials* **2021**, *14*, 3694, doi:10.3390/ma14133694.
52. Abdelkader, M.; Petrik, S.; Nestler, D.; Fijalkowski, M. Ceramics 3D Printing: A Comprehensive Overview and Applications, with Brief Insights into Industry and Market. *Ceramics* **2024**, *7*, 68–85, doi:10.3390/ceramics7010006.
53. Wu, H.; Liu, W.; Lin, L.; Li, Y.; Tian, Z.; Nie, G.; An, D.; Li, H.; Wang, C.; Xie, Z.; et al. Sintering Kinetics Involving Densification and Grain Growth of 3D Printed Ce–ZrO_2/Al_2O_3. *Materials Chemistry and Physics* **2020**, *239*, 122069, doi:10.1016/j.matchemphys.2019.122069.
54. Osama, A.; Fouda, N.; Eraky, M.T. Recent Advances in Design and Preparation of Bioceramic Materials for Manufacturing Dental Crowns by Vat Photopolymerization. *Discov Appl Sci* **2024**, *6*, doi:10.1007/s42452-024-06346-7.
55. Zhai, Z.; Qian, C.; Jiao, T.; Xu, C.; Sun, J. Zirconia Specimens Printed by Vat Photopolymerization: Mechanical Properties, Fatigue Properties, and Fractography Analysis. *Journal of Prosthodontics* **2024**, doi:10.1111/jopr.13942.

56. Yao, Y.; Cui, H.; Wang, W.; Xing, B.; Zhao, Z. High Performance Dental Zirconia Ceramics Fabricated by Vat Photopolymerization Based on Aqueous Suspension. *Journal of the European Ceramic Society* **2024**, *44*, 116795, doi:10.1016/j.jeurceramsoc.2024.116795.
57. Cho, M.-H.; Seol, H.-J. Effect of High-Speed Sintering on the Optical Properties, Microstructure, and Phase Distribution of Multilayered Zirconia Stabilized with 5 Mol% Yttria. *Materials* **2023**, *16*, 5570, doi:10.3390/ma16165570.
58. Nonaka, K.; Takeuchi, N.; Morita, T.; Pezzotti, G. Evaluation of the Effect of High-Speed Sintering on the Mechanical and Crystallographic Properties of Dental Zirconia Sintered Bodies. *Journal of the European Ceramic Society* **2023**, *43*, 510–520, doi:10.1016/j.jeurceramsoc.2022.10.044.
59. Sarthak, K.; Singh, K.; Bhavya, K.; Gali, S. Glazing as a Bonding System for Zirconia Dental Ceramics. *Materials Today: Proceedings* **2023**, *89*, 24–29, doi:10.1016/j.matpr.2023.04.308.
60. Hayashi, T.; Asakura, M.; Koie, S.; Hasegawa, S.; Mieki, A.; Aimu, K.; Kawai, T. In Vitro Study of Zirconia Surface Modification for Dental Implants by Atomic Layer Deposition. *IJMS* **2023**, *24*, 10101, doi:10.3390/ijms241210101.
61. Nazarov, D.; Kozlova, L.; Rogacheva, E.; Kraeva, L.; Maximov, M. Atomic Layer Deposition of Antibacterial Nanocoatings: A Review. *Antibiotics* **2023**, *12*, 1656, doi:10.3390/antibiotics12121656.
62. Binici Aygün, E.; Kaynak Öztürk, E.; Tülü, A.B.; Turhan Bal, B.; Karakoca Nemli, S.; Bankoğlu Güngör, M. Factors Affecting the Color Change of Monolithic Zirconia Ceramics: A Narrative Review. *JFB* **2025**, *16*, 58, doi:10.3390/jfb16020058.
63. Incesu, E.; Yanikoglu, N. Evaluation of the Effect of Different Polishing Systems on the Surface Roughness of Dental Ceramics. *The Journal of Prosthetic Dentistry* **2020**, *124*, 100–109, doi:10.1016/j.prosdent.2019.07.003.
64. Liu, X.; Aarts, J.; Ma, S.; Choi, J. The Influence of Polishing on the Mechanical Properties of Zirconia—A Systematic Review. *Oral* **2023**, *3*, 101–122, doi:10.3390/oral3010010.
65. Jakovac, M.; Živko-Babić, J.; Ćurković, L.; Aurer, A. Measurement of Ion Elution from Dental Ceramics. *Journal of the European Ceramic Society* **2006**, *26*, 1695–1700, doi:10.1016/j.jeurceramsoc.2005.03.242.
66. Chevalier, J.; Gremillard, L. Ceramics for Medical Applications: A Picture for the next 20 Years. *Journal of the European Ceramic Society* **2009**, *29*, 1245–1255, doi:10.1016/j.jeurceramsoc.2008.08.025.
67. Tian, J.-M.; Ho, W.-F.; Hsu, H.-C.; Song, Y.; Wu, S.-C. Evaluation of Feasibility on Dental Zirconia—Accelerated Aging Test by Chemical Immersion Method. *Materials* **2023**, *16*, 7691, doi:10.3390/ma16247691